Inorganica Chimica Acta, 196 (1992) 43–48

Low-spin iron(III) complexes of a tetradentate bis-amide ligand and X-ray crystal structure of *trans*-$[Fe(bpc)(1\text{-}MeIm)_2]ClO_4$ (H_2bpc = 4,5-dichloro-1,2-bis(2-pyridinecarboxamido)benzene; 1-MeIm = 1-methylimidazole)

Chi-Ming Che*, Wa-Hung Leung, Chi-Keung Li
Department of Chemistry, University of Hong Kong, Pokfulam Road, Hong Kong (Hong Kong)

Hei-Ying Cheng and Shie-Ming Peng
Department of Chemistry, National Taiwan University, Taipei (Taiwan)

(Received November 8, 1991; revised March 2, 1992)

Abstract

A series of low-spin iron(III) complexes $[Fe(bpc)(L)_2]^+$ (H_2bpc = 4,5-dichloro-1,2-bis(2-pyridinecarboxamido)benzene; L = Bu_3P, Im, 1-MeIm, ^{t}Bupy) have been synthesized. These iron complexes display reversible one-electron oxidation and reduction couples. The stable one-electron-oxidized species $[Fe(bpc)(Bu_3P)_2]^{2+}$ has been generated electrochemically. The complex *trans*-$[Fe(bpc)(1\text{-}MeIm)_2](ClO_4)$ has been characterized by X-ray crystallography: space group $P\bar{1}$; $a = 8.425(1)$, $b = 9.512(1)$, $c = 18.413(19)$ Å; $\alpha = 96.91(4)$, $\beta = 95.83(4)$, $\gamma = 90.44(1)°$; $V = 1457(2)$ Å^3; $Z = 2$.

Introduction

It is well known that iron complexes are involved in many biological reactions, such as the damage of DNA by bleomycins [1] and dioxygen activation by monooxygenase and dioxygenase [2]. Thus the design of iron complexes having simple organic ligands is of considerable importance because such attempts would allow precise structure determination and correlation between the structure and various spectroscopic properties.

In the absence of strong field ligands, iron(III) complexes are usually high spin in their electronic ground states. Recent works by us [3] and others [4–6] indicated that the deprotonated form of an organic amide is a good σ donor which forms stable complexes with transition metal ions. Herein is described the synthesis, spectral and redox properties of some low-spin iron(III) complexes of a tetradentate ligand H_2bpc and the molecular structure of *trans*-$[Fe(bpc)(1\text{-}MeIm)_2](ClO_4)$ (H_2bpc = 4,5-dichloro-1,2-bis(2-pyridinecarboxamido)benzene; 1-MeIm = 1-methylimidazole). Since the completion of this work, Valentine and co-workers reported the structure and catalytic activities of a related iron(III) bisamide complex $[Fe(bpb)Cl_2]^-$ (H_2bpb = 1,2-bis(2-pyridinecarboxamide)benzene) [7].

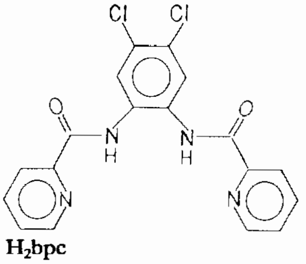

H_2bpc

Experimental

Physical measurements

UV–Vis spectra were obtained on a Shimadzu UV-240 spectrophotometer. IR spectra were obtained as nujol mulls on a Nicolet 20SXC FTIR spectrophotometer. Magnetic susceptibility was determined by Gouy's method using $Hg[Co(SCN)_4]$ as calibrant. Elemental analyses were performed by Butterworth Laboratories Ltd.

Electrochemistry

Acetonitrile (AR, Ajax) was distilled from $KMnO_4$ and CaH_2. Tetrabutylammonium fluoroborate (Southwestern analytical chemicals) was dried *in vacuo* at 100 °C. Cyclic voltammetry and constant potential electrolysis were performed on a Princeton Applied Re-

---

*Author to whom correspondence should be addressed.

0020-1693/92/$5.00

© 1992 – Elsevier Sequoia. All rights reserved

search model 173/179 potentiostat/digital coulometer equipped with a model 175 universal programmer. The working electrode was glassy carbon.

X-ray structure determination

Crystals of *trans*-[Fe(bpc)(1-MeIm)$_2$](ClO$_4$) were obtained by slow diffusion of diethyl ether into an acetonitrile solution of *trans*-[Fe(bpc)(1-MeIm)$_2$](ClO$_4$). Details of crystal parameters, data collection, and structure refinment are given in Table 1. Raw intensities were collected on a Nonius CAD4 fully automated four-circle diffractometer (graphite-monochromatized Mo Kα radiation) using the $\omega/2\theta$ scan mode at 297 K with $2\theta_{max}=50°$. Cell dimensions were obtained from 25 reflections with 2θ angle in the range of 20.00–28.86°. All reflections were corrected for Lorentz, polarization and absorption effect. All data reduction and structure refinement were performed using the NRCC-SDP-VAX packages. The structure was solved by the Patterson method and refined by least-squares; all non-hydrogen atoms were refined with anisotropic thermal parameters and hydrogen atoms were included at idealized positions with a fixed contribution. Tables 2 and 3 list the atomic coordinates of non-hydrogen atoms, and bond lengths and bond angles, respectively.

Materials

Ferric chloride (AR, BDH), 4,5-dichlorophenylenediamine (Aldrich) and picolinic acid (Aldrich) were used as received. The ligand H$_2$bpc was prepared by a modified procedure of Vagg's method [6]. All solvents and chemicals for syntheses were of reagent grade.

Syntheses

[Fe(bpc)(H$_2$O)Cl]

To a methanolic solution of H$_2$bpc (0.5 g in 50 ml) was added FeCl$_3$ (0.5 g) and CH$_3$CO$_2$Na (0.2 g). The resulting mixture was refluxed for 15 min and filtered. Upon standing at room temperature, a green solid

TABLE 1. Crystal data, details of intensity measurement and structure refinement of [Fe^{III}(bpc)(MeIm)$_2$](ClO$_4$)

Crystal data	
Empirical formula	C$_{26}$H$_{22}$O$_6$N$_8$Cl$_3$Fe
Formula weight	704.71
System	triclinic
a (Å)	8.425(1)
b (Å)	9.512(1)
c (Å)	18.413(19)
α (°)	96.91(4)
β (°)	95.83(4)
γ (°)	90.44(1)
V (Å^3)	1457(2)
Space group	$P\bar{1}$
Z	2
D_c (g cm^{-3})	1.606
μ (mm^{-1})	0.85
F(000)	718
Temperature (K)	297
Data collection, reduction, solution and refinement	
Radiation	Mo Kα ($l=0.70930$ Å)
Scan range	$0.65+0.35 \tan \theta$
Scan speed (°/min)	1.6–8.2
Crystal dimensions (mm)	$0.05\times0.25\times0.50$
Range h, k, l	-10 to 9 0 to 11 -21 to 21
Control reflections (standards)	3 (4% isotropic decay, data were corrected)
Total no. reflections	5482
No. unique reflections	5097
No. reflections with $I>2\sigma(I)$	3866
No. atoms and parameters refined	66, 398
Transmission factor: max., min.	1.00, 0.89
Residual electron density: max., min. (e Å^{-3})	0.74, -0.71
R^a	0.046
R'^b	0.043
S^c	3.21

$^aR=\Sigma(|F_o|-|F_c|)/\Sigma|F_o|$. $^bR'=[\Sigma(w||F_o|-|F_c||^2)/\Sigma w|F_o|^2]^{1/2}$. $^cS=[\Sigma(w||F_o|-|F_o||^2)/(n-p)]^{1/2}$; n is the number of observed reflections, p is the number of parameters used.

TABLE 2. Atomic parameters x, y, z and B_{iso} (the mean of the principal axes of the thermal ellipsoid); e.s.d.s refer to the last digit printed

	x	y	z	B_{iso}
Fe	0.92172(8)	0.68748(7)	0.23428(3)	2.135(25)
Cl(1)	0.69516(15)	0.98377(13)	−0.07452(6)	3.60(6)
Cl(2)	0.98315(17)	0.79244(14)	−0.11733(6)	4.09(6)
N1	1.1029(4)	0.5739(4)	0.27273(18)	2.51(16)
N2	1.0346(4)	0.6714(3)	0.15020(17)	2.22(15)
N3	0.7846(4)	0.8018(3)	0.18038(17)	2.18(15)
N4	0.7614(4)	0.7236(4)	0.30718(18)	2.42(15)
N5	1.0412(4)	0.8591(3)	0.28195(18)	2.45(15)
N6	1.1499(5)	1.0300(4)	0.36319(20)	3.46(19)
N7	0.7997(4)	0.5116(4)	0.19544(18)	2.53(16)
N8	0.6492(5)	0.3620(4)	0.11717(20)	3.20(18)
C1	1.1408(6)	0.5365(5)	0.34060(24)	3.10(21)
C2	1.2793(6)	0.4667(5)	0.3589(3)	3.68(23)
C3	1.3821(6)	0.4322(5)	0.3071(3)	3.86(24)
C4	1.3454(6)	0.4701(5)	0.2376(3)	3.83(24)
C5	1.2076(5)	0.5414(5)	0.22242(23)	2.69(20)
C6	1.1660(5)	0.5928(5)	0.14880(23)	2.92(20)
C7	0.9615(5)	0.7390(4)	0.09189(21)	2.22(18)
C8	1.0098(5)	0.7320(5)	0.02195(23)	2.60(19)
C9	0.9257(5)	0.8071(5)	−0.02927(22)	2.59(19)
C10	0.7983(5)	0.8896(4)	−0.01084(22)	2.34(18)
C11	0.7466(5)	0.8937(4)	0.05906(22)	2.27(18)
C12	0.8274(5)	0.8164(4)	0.11008(21)	2.19(18)
C13	0.6650(5)	0.8681(4)	0.21275(23)	2.65(19)
C14	0.6502(5)	0.8158(5)	0.28604(22)	2.60(19)
C15	0.5263(6)	0.8567(5)	0.3265(3)	3.82(24)
C16	0.5124(6)	0.7969(6)	0.3911(3)	4.2(3)
C17	0.6217(6)	0.7013(5)	0.41142(23)	3.30(22)
C18	0.7452(6)	0.6666(5)	0.36964(23)	2.92(20)
C19	1.1037(6)	0.9617(5)	0.24604(25)	3.86(24)
C20	1.1697(7)	1.0666(5)	0.2953(3)	4.4(3)
C21	1.0729(6)	0.9053(5)	0.35266(23)	3.10(21)
C22	1.2039(7)	1.1114(5)	0.4341(3)	5.2(3)
C23	0.7731(6)	0.3905(5)	0.22823(25)	3.12(21)
C24	0.6801(6)	0.2990(5)	0.1801(3)	3.37(23)
C25	0.7229(6)	0.4890(5)	0.12897(24)	3.01(21)
C26	0.5523(7)	0.3068(6)	0.0493(3)	5.1(3)
O1	1.2481(4)	0.5633(4)	0.09794(18)	4.81(18)
O2	0.5742(4)	0.9560(4)	0.18957(17)	4.19(17)
Cl(3)	0.75858(21)	0.26927(18)	0.44164(8)	6.32(9)
O3	0.8207(8)	0.2032(7)	0.4956(3)	14.9(5)
O4	0.6240(8)	0.3369(9)	0.4544(4)	19.0(6)
O5	0.8598(9)	0.3517(9)	0.4216(6)	25.5(9)
O6	0.7442(15)	0.1886(10)	0.3820(4)	28.1(10)

TABLE 3. Bond distances and bond angles of [Fe(bpc)(1-MeIm)$_2$] (ClO$_4$)

Fe–N(1)	1.997(3)	N(8)–C(26)	1.460(6)
Fe–N(2)	1.889(4)	C(1)–C(2)	1.378(6)
Fe–N(3)	1.883(3)	C(2)–C(3)	1.365(7)
Fe–N(4)	2.003(4)	C(3)–C(4)	1.377(7)
Fe–N(5)	1.975(4)	C(4)–C(5)	1.370(6)
Fe–N(7)	1.976(4)	C(5)–C(6)	1.505(6)
Cl(1)–C(10)	1.729(4)	C(6)–O(1)	1.227(5)
Cl(2)–C(9)	1.729(4)	C(7)–C(8)	1.384(6)
N(1)–C(1)	1.348(5)	C(7)–C(12)	1.400(6)
N(1)–C(5)	1.354(6)	C(8)–C(9)	1.392(6)
N(2)–C(6)	1.341(5)	C(9)–C(10)	1.381(6)
N(2)–C(7)	1.408(5)	C(10)–C(11)	1.396(6)
N(3)–C(12)	1.401(5)	C(11)–C(12)	1.389(5)
N(3)–C(13)	1.345(5)	C(13)–C(14)	1.509(6)
N(4)–C(14)	1.348(5)	C(13)–O(2)	1.223(5)
N(4)–C(18)	1.348(5)	C(14)–C(15)	1.375(6)
N(5)–C(19)	1.373(5)	C(15)–C(16)	1.394(7)
N(5)–C(21)	1.323(6)	C(16)–C(17)	1.356(7)
N(6)–C(20)	1.364(6)	C(17)–C(18)	1.375(6)
N(6)–C(21)	1.331(6)	C(19)–C(20)	1.341(7)
N(6)–C(22)	1.464(6)	C(23)–C(24)	1.350(7)
N(7)–C(23)	1.390(5)	Cl(3)–O(3)	1.306(4)
N(7)–C(25)	1.318(6)	Cl(3)–O(4)	1.336(6)
N(8)–C(24)	1.370(6)	Cl(3)–O(5)	1.266(7)
N(8)–C(25)	1.338(6)	Cl(3)–O(6)	1.257(8)
N(1)–Fe–N(2)	82.17(15)	N(1)–C(5)–C(4)	122.7(4)
N(1)–Fe–N(3)	165.87(14)	N(1)–C(5)–C(6)	115.7(4)
N(1)–Fe–N(4)	111.48(15)	C(4)–C(5)–C(6)	121.6(4)
N(1)–Fe–N(5)	87.82(14)	N(2)–C(6)–C(5)	110.1(4)
N(1)–Fe–N(7)	90.32(14)	N(2)–C(6)–O(1)	128.6(4)
N(2)–Fe–N(3)	84.19(15)	C(5)–C(6)–O(1)	121.3(4)
N(2)–Fe–N(4)	166.16(14)	N(2)–C(7)–C(8)	125.9(4)
N(2)–Fe–N(5)	94.12(15)	N(2)–C(7)–C(12)	113.5(3)
N(2)–Fe–N(7)	90.33(15)	C(8)–C(7)–C(12)	120.7(4)
N(3)–Fe–N(4)	82.33(15)	C(7)–C(8)–C(9)	118.7(4)
N(3)–Fe–N(5)	89.52(14)	Cl(2)–C(9)–C(8)	118.2(3)
N(3)–Fe–N(7)	93.41(15)	Cl(2)–C(9)–C(10)	120.7(3)
N(4)–Fe–N(5)	88.88(15)	C(8)–C(9)–C(10)	121.1(4)
N(4)–Fe–N(7)	87.38(14)	Cl(1)–C(10)–C(9)	120.9(3)
N(5)–Fe–N(7)	174.91(14)	Cl(1)–C(10)–C(11)	118.8(3)
Fe–N(1)–C(1)	130.2(3)	C(9)–C(10)–C(11)	120.2(4)
Fe–N(1)–C(5)	112.2(3)	C(10)–C(11)–C(12)	119.1(4)
C(1)–N(1)–C(5)	117.3(4)	N(3)–C(12)–C(7)	113.8(3)
Fe–N(2)–C(6)	119.6(3)	N(3)–C(12)–C(11)	126.1(4)
Fe–N(2)–C(7)	113.9(3)	C(7)–C(12)–C(11)	120.1(4)
C(6)–N(2)–C(7)	126.3(3)	N(3)–C(13)–C(14)	110.0(3)
Fe–N(3)–C(12)	114.4(3)	N(3)–C(13)–O(2)	128.7(4)
Fe–N(3)–C(13)	119.2(3)	C(14)–C(13)–O(2)	121.3(4)
C(12)–N(3)–C(13)	126.2(3)	N(4)–C(14)–C(13)	115.9(4)
Fe–N(4)–C(14)	111.8(3)	N(4)–C(14)–C(15)	122.9(4)
Fe–N(4)–C(18)	130.5(3)	C(13)–C(14)–C(15)	121.2(4)
C(14)–N(4)–C(18)	117.6(4)	C(14)–C(15)–C(16)	118.5(4)
Fe–N(5)–C(19)	125.6(3)	C(15)–C(16)–C(17)	118.6(4)
Fe–N(5)–C(21)	129.5(3)	C(16)–C(17)–C(18)	120.4(4)
C(19)–N(5)–C(21)	104.8(4)	N(4)–C(18)–C(17)	121.9(4)
C(20)–N(6)–C(21)	106.8(4)	N(5)–C(19)–C(20)	109.7(4)
C(20)–N(6)–C(22)	126.6(4)	N(6)–C(20)–C(19)	106.8(4)
C(21)–N(6)–C(22)	126.5(4)	N(5)–C(21)–N(6)	111.8(4)
Fe–N(7)–C(23)	130.5(3)	N(7)–C(23)–C(24)	108.7(4)
Fe–N(7)–C(25)	123.8(3)	N(8)–C(24)–C(23)	106.9(4)
C(23)–N(7)–C(25)	105.7(4)	N(7)–C(25)–N(8)	111.5(4)
C(24)–N(8)–C(25)	107.2(4)	O(3)–Cl(3)–O(4)	114.7(4)
C(24)–N(8)–C(26)	128.1(4)	O(3)–Cl(3)–O(5)	111.3(5)
C(25)–N(8)–C(26)	124.7(4)	O(3)–Cl(3)–O(6)	111.1(6)
N(1)–C(1)–C(2)	122.2(4)	O(4)–Cl(3)–O(5)	110.9(5)
C(1)–C(2)–C(3)	119.8(4)	O(4)–Cl(3)–O(6)	112.3(7)
C(2)–C(3)–C(4)	118.8(4)	O(5)–Cl(3)–O(6)	94.8(8)
C(3)–C(4)–C(5)	119.3(4)		

precipitated gradually, which was filtered and washed with methanol (yield 50%). *Anal.* Calc. for [Fe-$C_{18}H_{12}N_4O_3Cl_3$]: C, 43.7; H, 2.42; N 11.4; Cl, 21.6. Found: C, 43.4; H, 2.54; N, 11.3; Cl, 21.6%.

[Fe(bpc)(PBu$_3$)$_2$](ClO$_4$)

A mixture of H$_2$bpc (0.5 g), FeCl$_3$ (0.5 g) and CH_3CO_2Na (0.2 g) in methanol (30 ml) was heated for 15 min. It was filtered and further refluxed with tri-n-butylphosphine (0.2 g) for 10 min. Upon addition of LiClO$_4$, a green solid was precipitated, which was filtered and washed with methanol (yield 70%). UV–Vis (CH_3CN) λ_{max} (nm) (log ϵ): 750br (3.24), 610 (3.15), 320 (4.21), 270 (4.34). μ_{eff} (solid sample) = 1.85 μ_B at 298 K. *Anal.* Calc. for [$FeC_{42}H_{64}N_4Cl_2O_2P_2$]: C, 53.4; H, 6.78; N, 5.93. Found: C, 53.5; H, 6.92; N, 6.11%.

[Fe(bpc)(1-MeIm)$_2$]ClO$_4$ (1-MeIm = 1-methylimidazole)

This was prepared by a procedure similar to that for [Fe(bpc)(PBu_3)$_2$]ClO_4 but using 1-methylimidazole instead of tri-n-butylphosphine (yield 70%). UV–Vis (CH_3CN) λ_{max} (nm) (log ϵ): 740br (3.26), 350 (4.17), 265(4.48). μ_{eff} (solid sample) = 1.79 μB at 298 K. *Anal.* Calc. for [$FeC_{34}H_{22}N_8Cl_3O_6$]: C, 44.3; H, 3.12; N, 15.9. Found: C, 44.8; H, 3.10; N, 16.2%.

[Fe(bpc)(Im)$_2$](ClO$_4$) (Im = imidazole)

This was prepared by a procedure similar to that for [Fe(bpc)(PBu_3)$_2$]ClO_4 but using imidazole instead of tri-n-butylphosphine (yield 50%). UV–Vis (CH_3CN) λ_{max} (nm) (log ϵ): 740br (3.26), 410sh (3.70), 350 (3.99), 260 (4.31). *Anal.* Calc. for [$FeC_{24}H_{18}N_8O_6Cl_3$]: C, 42.6; H, 2.66; N, 16.6. Found: C, 42.2; H, 2.52; N, 16.5%.

[Fe(bpc)(^{t}Bupy)$_2$](ClO$_4$) (^{t}Bupy = 4-tert-butylpyridine)

This was prepared by a procedure similar to that for [Fe(bpc)(PBu_3)$_2$]ClO_4 but using 4-tert-butylpyridine instead of tri-n-butylphosphine (yield 60%). UV–Vis (CH_3CN) λ_{max} (nm) (log ϵ): 665br (3.02), 353 (4.07), 270 (4.31). *Anal.* Calc. for [$FeC_{36}H_{36}N_6O_6Cl_3$]: C, 53.3; H, 4.44; N, 10.4. Found: C, 53.1; H, 4.41; N, 10.3%.

[Fe(bpc)(PBu$_3$)$_2$]$^{2+}$

This was generated by constant potential oxidation of [Fe(bpc)(PBu_3)$_2$]$^+$ at 0.7 V versus Ag/$AgNO_3$ (0.1 M) in acetonitrile. UV–Vis (CH_3CN) λ_{max} (nm) (log ϵ): 580 (3.60), 320 (4.27), 270 (4.24).

Results and discussion

The ligand H_2bpc, in its deprotonated form, easily reacts with Fe(III) to form stable complexes. A similar result has also been reported by Valentine and co-workers [7]. Unlike [Fe(bpb)Cl_2]$^-$ which is high spin, [Fe(bpc)(L)$_2$](ClO_4) are low spin in their electronic ground states. The respective μ_{eff} of 1.85 and 1.79 μB at 298 K for [Fe(bpc)(PBu_3)$_2$](ClO_4) and [Fe(bpc)(1-MeIm)$_2$](ClO_4) are characteristic of the spin-only value for one unpaired electron.

The UV–Vis spectrum of [Fe(bpc)(PBu_3)$_2$]$^+$ is shown in Fig. 1. As with other [Fe(bpc)(L)$_2$]$^+$ complexes, the spectrum shows broad absorptions at 740–750 nm, which are due to ligand to metal charge transfer transitions. The intense absorption bands in the region 260–350 nm are mostly due to the intraligand $\pi \rightarrow \pi^*$ transitions. The IR spectrum of [Fe(bpc)(PBu_3)$_2$]ClO_4 shows ν(C=O) stretching at 1596 cm^{-1} which is lower than the value of 1620 cm^{-1} for the free H_2bpc ligand. This is attributed to the deprotonation of the ligand upon coordination to iron. Similar ν(C=O) stretching frequencies have been found in other [Fe(bpc)(L)$_2$]$^+$ complexes.

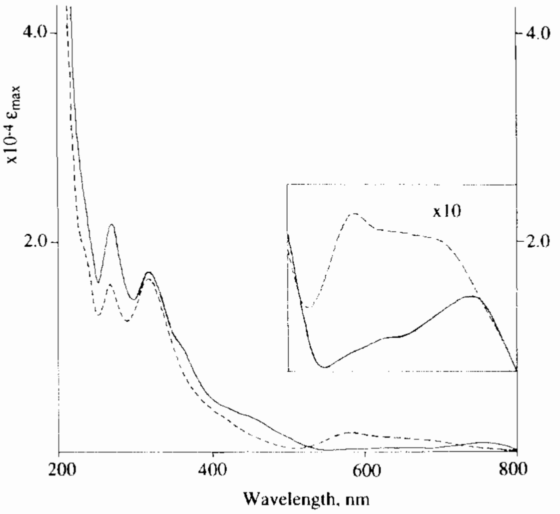

Fig. 1. UV–Vis absorption spectra of [Fe(bpc)(PBu_3)$_2$]$^+$ (——) and [Fe(bpc)(PBu_3)$_2$]$^{2+}$ (– – – –) in acetonitrile at room temperature.

Structure of [Fe(bpc)(1-MeIm)$_2$]ClO$_4$

There are few structures of iron(III)–amide complexes [4e, 7, 8]. An ORTEP drawing of the [Fe(bpc)(1-MeIm)$_2$]$^+$ cation is shown in Fig. 2. The coordination geometry around the iron atom is octahedral with the two 1-methylimidazole ligands *trans* to each other. The Fe(III)–N(pyridine) distances of 1.997(3)–2.003(4) Å are comparable to those values of 1.967(8)–1.980(8) Å in [Fe(phen)$_3$](ClO_4)$_3$·H_2O (phen = 1,10-phenanthroline) [9] and 1.981(4)–1.983(4) Å in [Fe(pypep)$_2$]Cl·2H_2O (Hpypep = *N*-(2-(4-imidazolyl)ethyl)pyridine-2-carboxamide) [8], but considerably shorter than the values of 2.178(5) and 2.173(5) Å in [Fe(bpb)Cl_2]$^-$ [7]. The Fe(III)–N(imidazole) distances of 1.975(4)–1.976(4) Å are similar to those of 1.989(8) and 1.990(16) Å found in the respective low-spin [Fe(TPP)(Im)$_2$]Cl (H_2TPP = *meso*-tetraphenylporphyrin) [10] and [Fe(Proto-IX)(1-MeIm)$_2$]ClO_4 (Proto-IX = protoporphyrin IX) [11] systems. The measured Fe(III)–N(amide) distances are 1.883(3)–1.889(4) Å. Similar values of 1.957(4) Å in [Fe(pypep)$_2$]Cl·2H_2O [8] and 1.879(7)–1.926(6) Å in the Fe(IV)–tetraamide complex [4e] have also been reported. A direct comparison between [Fe(bpc)(1-MeIm)$_2$]$^+$ and [Fe(bpb)Cl_2]$^-$ [7] reveals that the Fe–(pyridine) and Fe–(amide) distances of the former are considerably

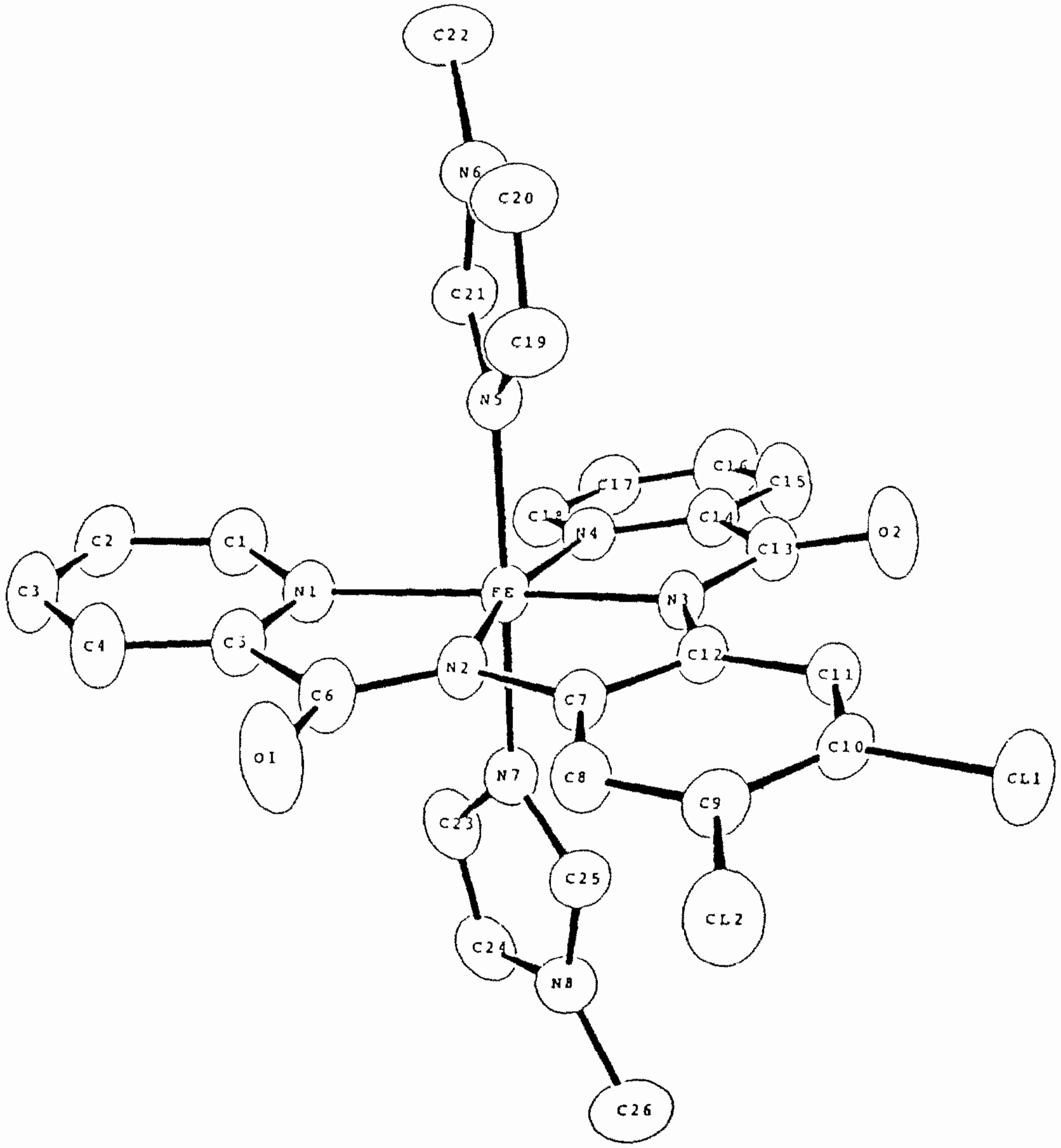

Fig. 2. ORTEP plot of the $[Fe(bpc)(1\text{-}MeIm)_2]^+$ cation.

shorter than the latter; this is understandable because of the high-spin nature of the latter complex. The bond lengths and angles of the bpc ligand are normal [12].

Electrochemistry

Figure 3 shows the cyclic voltammogram of $[Fe(bpc)(PBu_3)_2]^+$ in acetonitrile. Two reversible/quasi-reversible one-electron couples at 0.61 and −0.64 V versus ferrocenium–ferrocene were found. The reduction couple at −0.64 V is metal centred ($Fe(III) + e \rightarrow Fe(II)$) since the bpc ligand is electrochemically inactive in the potential range 0 to −1.5 V in acetonitrile [3a, 3b, 12]. Results of the scan rate dependence of the oxidation couple showed that the electrode reaction is a simple one-electron transfer process. Between scan rates of 20–200 mV/s, the peak to peak separation ΔE of 60–70 mV and the current function $i_{pa}/\nu^{1/2}$ are relatively independent of scan rates.

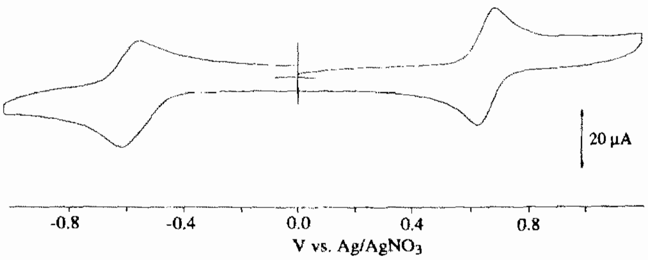

Fig. 3. Cyclic voltammogram of $[Fe(bpc)(PBu_3)_2]^+$ in acetonitrile. Working electrode, edge plane pyrolytic graphite; scan rate, 100 mV/s; supporting electrolyte, 0.1 M $[Bu_4N]BF_4$.

TABLE 4. Redox potentials of some Fe(III), Cr(III) and Co(III)–bpc complexes

Complex	$E°$ (V vs. $Cp_2Fe^{+/0}$)	
	Oxidation	Reduction
$[Fe(bpc)(PBu_3)_2](ClO_4)$	0.61	−0.64
$[Fe(bpc)(Im)_2](ClO_4)$	0.64	−0.57
$[Fe(bpc)(1\text{-}MeIm)_2](ClO_4)$	0.62	−0.54
$[Fe(bpc)(^tBupy)_2](ClO_4)$	0.58	
$[Co(bpc)(py)_2](ClO_4)^a$	0.91	−0.53
$[Cr(bpc)(^tBupy)_2](ClO_4)^b$	0.80	

Scan = 100 mV/s, Supporting electrolyte: 0.1 M $[Bu_4N]BF_4$ in CH_3CN. [a]Ref. 12. [b]Ref. 3e.

A similar electrochemistry has been found for other $[Fe(bpc)(L)_2]^+$ complexes. The electrochemical data are listed in Table 4. For $[Fe(bpc)(PBu_3)_2]^+$, constant potential coulometry at 0.7 V versus $Ag/AgNO_3$ showed that $n = 1.1$, establishing a one-electron oxidative process. The oxidized product was stable in acetonitrile and could be reduced back to the starting Fe(III) complex by hydrazine with over 95% recovery. Its UV–Vis spectrum shown in Fig. 1 has broad absorptions in the region 500–800 nm, which is characteristic of the cation radical of 1,2-diaminobenzene ring. A similar UV–Vis spectrum has also been found for the one-electron oxidized form of $[Co(bpb)(py)_2]^+$ [12]. From Table 4, it is obvious that the one-electron oxidation potentials of *trans*-$[Fe(bpc)(L)_2]^+$ (L = py, ^{t}Bupy) are about 150 mV lower than that for the isostructural Co(III) [12] and Cr(III) [3e] analogues. This may suggest that in the $[Fe(bpc)(L)_2]^+$ complexes, the redox orbital responsible for the oxidation has more contribution from the metal centre than that in the cases of Co(III) and Cr(III).

Acknowledgements

We acknowledge support from the University of Hong Kong and the National Science Council of Taiwan. W.H.L. is grateful for a studentship administered by the Croucher Foundation of Hong Kong.

Supplementary material

Tables of H-atom coordinates, thermal parameters and structure factors are available from the authors upon request.

References

1 J. C. Dabrowiak, *Adv. Inorg. Biochem.,* (1983) 4, and refs. therein.
2 T. J. McMurry and J. T. Groves, in P. R. Ortiz de Montellano (ed.), *Cytochrome P-450: Structure, Mechanism and Biochemistry,* Plenum, New York, 1986, pp. 1–28.
3 (a) C. M. Che and W. K. Cheng, *J. Chem. Soc., Chem. Commun.,* (1986) 1443; (b) C. M. Che, W. K. Cheng and T. C. W. Mak, *J. Chem. Soc., Chem. Commun.,* (1986) 200; (c) C. M. Che, J. X. Ma, W. T. Wong, T. F. Lai and C. K. Poon, *Inorg. Chem., 27* (1986) 2547; (d) S. T. Mak, V. W. W. Yam, C. M. Che and T. C. W. Mak, *J. Chem. Soc., Dalton Trans.,* (1990) 2555; (e) W. H. Leung, J. X. Ma, V. W. W. Yam, C. M. Che and C. K. Poon, *J. Chem. Soc., Dalton Trans.,* (1990) 1071.
4 (a) T. J. Collins, B. D. Santarsiero and G. H. Spies, *J. Chem. Soc., Chem. Commun.,* (1983) 681. (b) F. C. Anson, T. J. Collins, R. J. Coots, S. L. Gipson and T. G. Richmond, *J. Am. Chem. Soc., 106* (1984) 5037; (c) F. C. Anson, T. J. Collins, T. G. Richmond, B. D. Santarsiero, J. E. Toth and B. G. R. T. Treco, *J. Am. Chem. Soc., 109* (1987) 2974; (d) T. J. Collins, R. D. Powell, C. Slebodnick and E. S. Uffelman, *J. Am. Chem. Soc., 112* (1990) 899; (e) T. J. Collins, K. L. Kostka, E. Munck and E. S. Uffelman, *J. Am. Chem. Soc., 112* (1990) 5637.
5 (a) D. W. Margerum, *Pure Appl. Chem., 55* (1983) 23; (b) L. L. Diaddario, W. R. Robinson and D. W. Margerum, *Inorg. Chem., 22* (1983) 1021; (c) E. Kimura, *J. Coord. Chem., 15* (1983) 1; (d) L. Fabbrizzi, T. A. Kaden, A. Perotti, B. Seghi and L. Siegfried, *Inorg. Chem., 25* (1986) 321.
6 (a) R. L. Chapman, F. S. Stephens and R. S. Vagg, *Inorg. Chim. Acta, 52* (1981) 161; (b) M. Mulgi, F. S. Stephens and R. S. Vagg, *Inorg. Chim. Acta, 62* (1982) 215; (c) R. L. Chapman and R. S. Vagg, *Inorg. Chim. Acta, 33* (1979) 227.
7 Y. Yang, F. Diederich and J. S. Valentine, *J. Am. Chem. Soc., 113* (1991) 7195.
8 X. Tao, D. W. Stephan and P. K. Mascharak, *Inorg. Chem., 26* (1987) 754.
9 J. Baker, L. M. Engelhardt, B. M. Figgis and A. H. White, *J. Chem. Soc., Dalton Trans.,* (1975) 530.
10 D. M. Collins, R. Countryman and J. L. Hoard, *J. Am. Chem. Soc., 94* (1972) 2066.
11 R. G. Little, K. R. Dymock and J. A. Ibers, *J. Am. Chem. Soc., 97* (1975) 4532.
12 S. T. Mak, W. T. Wong, V. W. W. Yam, T. F. Lai and C. M. Che, *J. Chem. Soc., Dalton Trans.,* (1991) 1915.